Adaptive feed-forward hysteresis compensation for piezoelectric actuators

Arnfinn Aas Eielsen, Jan Tommy Gravdahl, and Kristin Y. Pettersen

Related Articles

Note: A resonant fiber-optic piezoelectric scanner achieves a raster pattern by combining two distinct resonances
Rev. Sci. Instrum. 83, 086102 (2012)

Characterization of piezoelectric ceramics and 1-3 composites for high power transducers
Appl. Phys. Lett. 101, 032902 (2012)

Origin of multiple memory states in organic ferroelectric field-effect transistors
Appl. Phys. Lett. 101, 033304 (2012)

Origin of multiple memory states in organic ferroelectric field-effect transistors
APL: Org. Electron. Photonics 5, 153 (2012)

Cantilever driving low frequency piezoelectric energy harvester using single crystal material
$0.71Pb(Mg_{1/3}Nb_{2/3})O3-0.29PbTiO3$
Appl. Phys. Lett. 101, 033502 (2012)

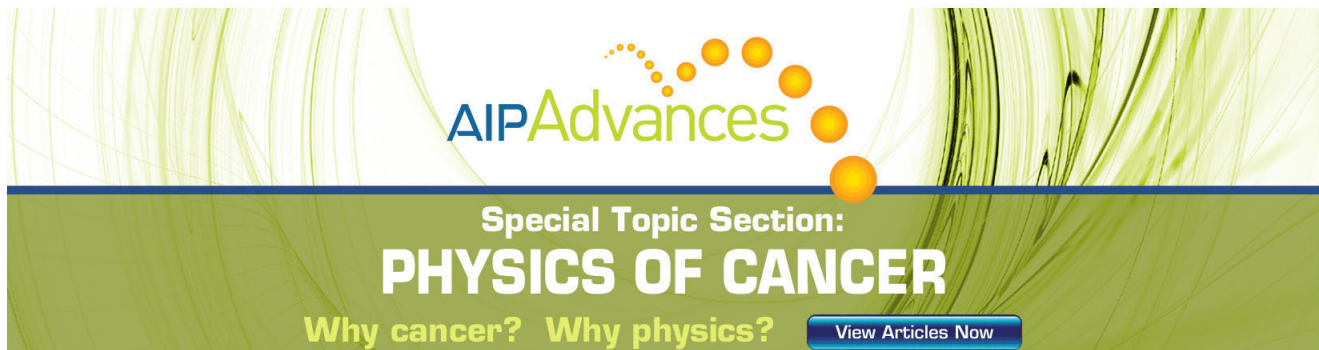## Additional information on Rev. Sci. Instrum.

Journal Homepage: http://rsi.aip.org
Journal Information: http://rsi.aip.org/about/about_the_journal
Top downloads: http://rsi.aip.org/features/most_downloaded
Information for Authors: http://rsi.aip.org/authors

Adaptive feed-forward hysteresis compensation for piezoelectric actuators

Arnfinn Aas Eielsen,[a)] Jan Tommy Gravdahl,[b)] and Kristin Y. Pettersen[c)]
Department of Engineering Cybernetics, Norwegian University of Science and Technology, Trondheim, Norway

Piezoelectric actuators are often employed for high-resolution positioning tasks. Hysteresis and creep nonlinearities inherent in such actuators deteriorate positioning accuracy. An online adaptive non-linear hysteresis compensation scheme for the case of symmetric hysteretic responses and certain periodic reference trajectories is presented. The method has low complexity and is well suited for real-time implementation. Experimental results are presented in order to verify the method, and it is seen that the error due to hysteresis is reduced by more than 90% compared to when assuming a linear response. © *2012 American Institute of Physics*. [http://dx.doi.org/10.1063/1.4739923]

I. INTRODUCTION

Micro- and nanopositioning devices often employ piezo-electric actuators. Such actuators provide a fast and friction free response, and the resolution is only limited by instrumentation noise. For low-speed reference trajectory tracking, the largest error contribution comes from the hysteresis and creep nonlinearities.[1,2] The error introduced by these nonlinearities can be reduced by using feed-forward or feedback control, or by driving the actuator by charge rather than voltage.

Due to hysteresis, the average gain of a piezoelectric actuator depends on the amplitude of the driving voltage.[3] The observed piezoelectric response also changes over time, as the gain is dependent on temperature variations and depolarization, as well as other factors.[4] Feedback control effectively reduces the sensitivity to such uncertainty, as well as the disturbance introduced by hysteresis, if integral action is used.[5] The reduction in error when using feedback control is dependent on the obtainable closed-loop bandwidth, but high bandwidth control also increases the overall noise in the system.[6,7]

By using a feed-forward scheme in addition to feedback control, better tracking performance can be obtained. For reduction of the error introduced by hysteresis, there are several methods based on inversion of the Preisach model, or variants thereof.[8,9] In general, performance when using feed-forward control depends directly on the accuracy of the model.[10] In the presence of uncertainties and changing responses, on-line adaptation can be used to improve the accuracy.[9] Such models tend to be large if an accurate description is required, and can therefore be computationally demanding.

Driving a piezoelectric actuator using charge rather than voltage is known to provide excellent suppression of hysteresis.[11,12] Even though the hysteresis disturbance can be suppressed, driving the piezoelectric actuator using charge will not remove the uncertainty in actuator gain. Also, charge drives are often not a part of existing instrumentation configurations, as voltage drives have been the standard choice for positioning tasks when using piezoelectric actuators.

In this paper, an online adaptive nonlinear feed-forward hysteresis compensation scheme is presented. It is suitable for symmetric hysteretic responses and certain periodic reference trajectories. Being adaptive, the method retains good accuracy in the presence of uncertainties in the response, both with regards to the gain and the shape of the hysteretic response. The method has low complexity and is amenable to real-time implementation.

Furthermore, experimental results are presented to verify and illustrate the theoretical result. The presented method is then applied to a standard instrumentation configuration, utilizing a capacitive displacement sensor and a voltage drive. In the experiments, it is seen that the error due to hysteresis can be reduced by more than 90% compared to when assuming a linear response. It should be noted that it is straightforward to augment the method using, e.g., an integral control law to further reduce the tracking error, although this is not discussed further in this paper.

The paper is organized as follows. In Sec. II, models for the ideal linear response and for the hysteretic response are presented. In Sec. III, two feed-forward schemes are described, one assuming an ideal linear response, and a scheme to compensate for the hysteretic behavior, based on the hysteresis model from Sec. II. The experimental results when applying the two feed-forward schemes are presented in Sec. IV. Appendices A, B, and C are provided to describe the details of the parameter identification scheme used, and the details of the derivation of the hysteresis compensation scheme.

II. SYSTEM MODEL

In this section, models for the system are presented. The system at hand is a flexure based nanopositioning stage with a piezoelectric stack actuator. Using an input signal with a low fundamental frequency, the system response can be described using a hysteresis model and a simple mechanical model.

A. Hysteresis model

The hysteretic behavior of piezoelectric actuators is due to ferroelectric loss phenomena. The hysteresis exhibited in such actuators will appear between applied voltage and induced charge.[11] The force developed by the actuator will

---
a)Electronic mail: arnfinn.aas.eielsen@itk.ntnu.no.
b)Electronic mail: jan.tommy.gravdahl@itk.ntnu.no.
c)Electronic mail: kristin.y.pettersen@itk.ntnu.no.

therefore exhibit hysteresis when driving such actuators using voltage.

A phenomenological model that can be used to describe the hysteresis in piezoelectric actuators is the Coleman-Hodgdon model,[13] which is given as

$$\dot{w} = \beta \dot{u} - \alpha w |\dot{u}| + \gamma |\dot{u}| u, \quad w(0) = w_0, \tag{1}$$

where u is the input, and w is the output. The parameters must satisfy the conditions $\alpha > 0$, $\beta > 0$, $\frac{\gamma}{\alpha} > \beta$, and $\frac{\gamma}{\alpha} \leq 2\beta$ in order for the model to yield a response that is in accordance with the laws of thermodynamics.[14] This means that the slope $\dot{w}$ will have the same sign as the slope $\dot{u}$, that is $\frac{dw}{du} > 0$. This is the same as saying that the output will never move in the opposite direction of the input.

The input-output map generated by the model (1) has a symmetric stationary response to periodic inputs, which are monotonically increasing and decreasing between two extrema. The model is therefore best suited to describe hysteretic responses that are dominantly symmetric, and for such periodic input signals. The solution of the model is defined, however, for a larger class of input signals. The input signal u must be bounded, piecewise continuous, and connected. This also implies that the time derivative $\dot{u}$ exists and is bounded, i.e., $u \in C^0$. This includes signals such as triangle-waves or low-pass filtered steps and square-waves, but not unfiltered steps and square-waves.

The hysteresis model (1) can also be expressed in a different form, with an identical input-output response. That is, the output w can be found from

$$w = cu + w_h, \tag{2}$$

where w_h is the solution to

$$\dot{w}_h = -b\dot{u} - aw_h|\dot{u}|, \quad w_h(0) = w_{h0}. \tag{3}$$

The parameters in this formulation can be found using the parameters in (1), and the relations are

$$a = \alpha, \quad b = \frac{\gamma - \alpha\beta}{\alpha}, \quad \text{and } c = \frac{\gamma}{\alpha}. \tag{4}$$

The derivation of the expressions in (2), (3), and (4) can be found in Appendix B.

The alternative model formulation in (2) and (3) will be used to develop a hysteresis compensation scheme in Sec. III B.

B. Mechanical model

The dynamics of a well designed nanopositioning stage can be accurately approximated as a linear mass-spring-damper system. For the displacement of a point x on the mechanical structure, the dynamics is therefore described by

$$m\ddot{x} + d\dot{x} + kx = f, \tag{5}$$

where m is the mass of the moving platform, d is the damping coefficient, k is the spring constant, and f is the force developed by the actuator.

Here, it is assumed that reference trajectories, r, will have a fundamental frequency below approximately 1% of the natural undamped frequency $\omega_0 = \sqrt{k/m}$, and that the contribution of the damping and inertial forces therefore can be ne-
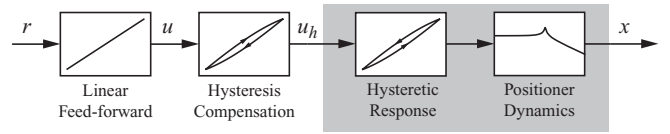

FIG. 1. Feed-forward tracking control scheme.

glected, i.e., $d\dot{x} \approx 0$ and $m\ddot{x} \approx 0$. The forces depending on the velocity and acceleration of the moving platform will be relatively small when the movements are slow, that is, the higher frequency components of the reference signal will be small close to the resonant frequency of the mechanical structure. The displacement x is therefore taken to be given by Hooke's law

$$x = \frac{1}{k}f. \tag{6}$$

Ideally, the actuator has a linear response, which is the standard assumption.[15] In that case, the force developed by the actuator should be

$$f = k_a u, \tag{7}$$

where k_a is the voltage-to-force gain coefficient. The relation between the applied voltage u and the displacement x, will then be according to (6),

$$x = \frac{k_a}{k}u = Ku, \tag{8}$$

where the lumped parameter K, a voltage-to-displacement gain coefficient, is introduced for convenience.

Since the actuator response is actually hysteretic, using the hysteresis model (1), or equivalently (2), provides a more accurate description of the observed displacement. The displacement will therefore, in this paper, be taken to be the output of the hysteresis model, i.e.,

$$x = w. \tag{9}$$

III. FEED-FORWARD TRACKING CONTROL

The objective for a tracking control scheme applied to a nanopositioning stage is to force the displacement x to follow a specified reference trajectory r. In order to achieve this, feed-forward and feedback control can be used. Feed-forward techniques can be very effective if an invertible and accurate system model can be found. Applying feedback will typically reduce sensitivity to model errors and unknown disturbances, but at the expense of a higher overall noise level.

For positioning devices utilizing piezoelectric actuators, when using reference trajectories with low fundamental frequencies, the disturbance due to hysteresis is the main source of error. In this section, two feed-forward schemes will be described. The first is simply assuming that the system has a linear response. The second scheme provides a method for inverting the response of the hysteresis model (1). The overall scheme is illustrated in Fig. 1.

A. Linear feed-forward

Assuming that the response of the system is linear, such as in (8),

$$x = Ku, \tag{10}$$

the applied voltage signal u should be

$$u = \frac{1}{K}r, \tag{11}$$

in order to achieve tracking.

Due to creep and hysteresis, the gain K will depend on the amplitude of the input signal u. Other effects also affect the observed gain, such as actuator temperature and depolarization. An estimate of the gain, $\hat{K}$, can be found from input-output data using, e.g., the least-squares method. Depending on the positioning device, the gain can change significantly. For the positioning device used in the experiments in Sec. IV, a relative change of more than 150% was observed from the minimal observable displacement to the maximal displacement.

As the gain changes depend on the input signal, using a static gain estimate $\hat{K}$ for feed-forward control can result in very large errors. In order to minimize the error for all reference signals, an online estimate of K should be used. This can be achieved by using the recursive least-squares method with the model (8) on the form

$$z = \theta\varphi, \tag{12}$$

where $z = x$, $\theta = K$, and $\varphi = u$. The parameter identification scheme is described in detail in Appendix A.

B. Hysteresis compensation

In this section, a feed-forward scheme that takes into account the hysteresis is presented. The scheme is based on inverting the response of the hysteresis model (1). Using the relations in (2) and (9), but defining a new input signal u_h, that is,

$$x = cu_h + w_h, \tag{13}$$

the above relation can be linearized by choosing the input signal

$$u_h = \frac{K}{c}u - \frac{1}{c}\hat{w}_h, \tag{14}$$

where $\hat{w}_h$ is an estimate of the term w_h. By substituting (14) into (13), the linear relationship between voltage u and the expression for the displacement as given in (8) is recovered,

$$x = cu_h + w_h = c\left(\frac{K}{c}u - \frac{1}{c}\hat{w}_h\right) + w_h = Ku, \tag{15}$$

if $\hat{w}_h = w_h$. Thus, generating an input signal using (11) and applying (14), the error introduced by the hysteresis is removed. In order for this to work, an estimate of w_h is required.

Assuming the parameters of the hysteresis model (1) are known, and the new set of parameters is found from the relations in (4), an estimate of w_h when using the new input signal u_h can be found by substituting (14) into (3), that is,

$$\dot{\hat{w}}_h = -b\dot{u}_h - a\hat{w}_h|\dot{u}_h|$$

$$= -b\left(\frac{K}{c}\dot{u} - \frac{1}{c}\dot{\hat{w}}_h\right) - a\hat{w}_h\left|\frac{K}{c}\dot{u} - \frac{1}{c}\dot{\hat{w}}_h\right|. \tag{16}$$

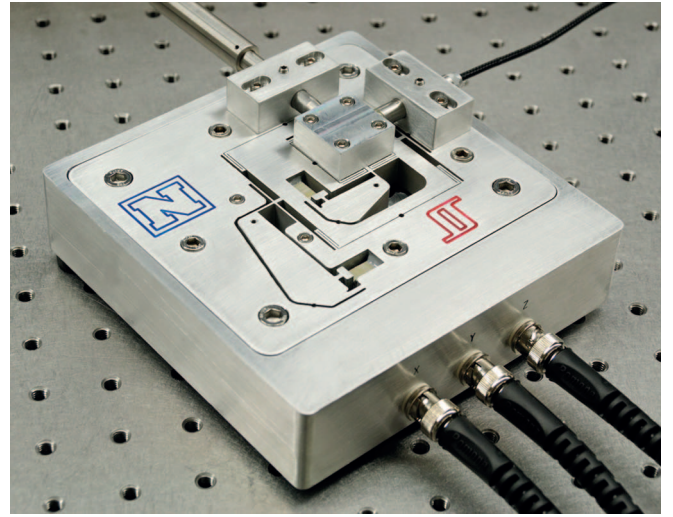
FIG. 2. Nanopositioning stage.

In Appendix C, it is shown that solving (16) is equivalent to solving

$$\dot{\hat{w}}_h = \begin{cases} K\frac{-a\hat{w}_h-b}{-a\hat{w}_h-b+c}\dot{u}, & \dot{u} \geq 0 \\ K\frac{a\hat{w}_h-b}{a\hat{w}_h-b+c}\dot{u}, & \dot{u} < 0 \end{cases}, \quad \hat{w}_h(0) = \hat{w}_{h0}. \tag{17}$$

The initial value $\hat{w}_{h0}$ can in principle be chosen arbitrarily. For the case of periodic inputs which are monotonically varying between two extrema, the solution will converge to a stationary input-output map after some cycles of the input signal. Assuming the system is at rest in an equilibrium where $u(0) = 0$ and $w(0) = 0$ when starting the integration, the initial value will be $\hat{w}_{h0} = 0$.

Inspecting (1), it can be seen that the parameters appear affinely with signals comprising of u and w and their time derivatives, i.e., the model can be put on the form

$$z = \theta^{\mathrm{T}}\varphi, \tag{18}$$
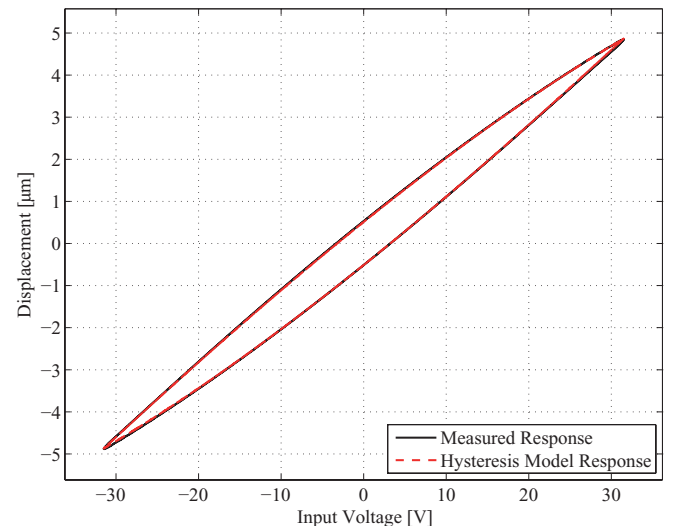

FIG. 3. The input-output map when using a 5 Hz triangle wave reference signal with 5 μm amplitude.

TABLE I. Identified parameters for the stationary response of the hysteresis model (1) and the linear approximation (8).

Reference signal	α	β	γ	K
2.5 μm @ 5.0 Hz	3.26×10^{-2}	1.36×10^{-1}	5.96×10^{-3}	0.141
5.0 μm @ 2.5 Hz	1.91×10^{-2}	1.49×10^{-1}	4.05×10^{-3}	0.156
5.0 μm @ 5.0 Hz	2.10×10^{-2}	1.47×10^{-1}	4.29×10^{-3}	0.155
7.5 μm @ 5.0 Hz	1.59×10^{-2}	1.55×10^{-1}	3.55×10^{-3}	0.165
Filtered PRBS	3.32×10^{-2}	1.36×10^{-1}	6.15×10^{-3}	0.154

where

$$\theta = (\alpha, \beta, \gamma)^{\mathrm{T}}, \tag{19}$$

$$\varphi = (-w|\dot{u}|, \dot{u}, |\dot{u}|u)^{\mathrm{T}}, \tag{20}$$

and $z = \dot{w}$. Here, θ is the called the parameter vector and φ the regressor. Having the model on the form (18) enables the usage of the recursive least-squares method to find the parameters in θ, as the displacement $x = w$ can be measured, and the the applied voltage u and the time derivative $\dot{u}$ are known and defined. The relations in (4) can then be used to find the parameters to be used in this hysteresis compensation scheme. The parameters in the model given by (2) and (3) cannot be identified, as it is not possible to measure the signal w_h. The parameter identification scheme is described in detail in Appendix A.

IV. RESULTS

A. Experimental setup

The experimental setup consisted of a dSPACE DS1103 hardware-in-the-loop system, an ADE 6810 capacitive gauge, and an ADE 6501 capacitive probe from ADE Technologies, a Piezodrive PDL200 voltage amplifier, the custom-made long-range serial-kinematic nanopositioner from EasyLab (see Fig. 2), two SIM 965 programmable filters, and a SIM983
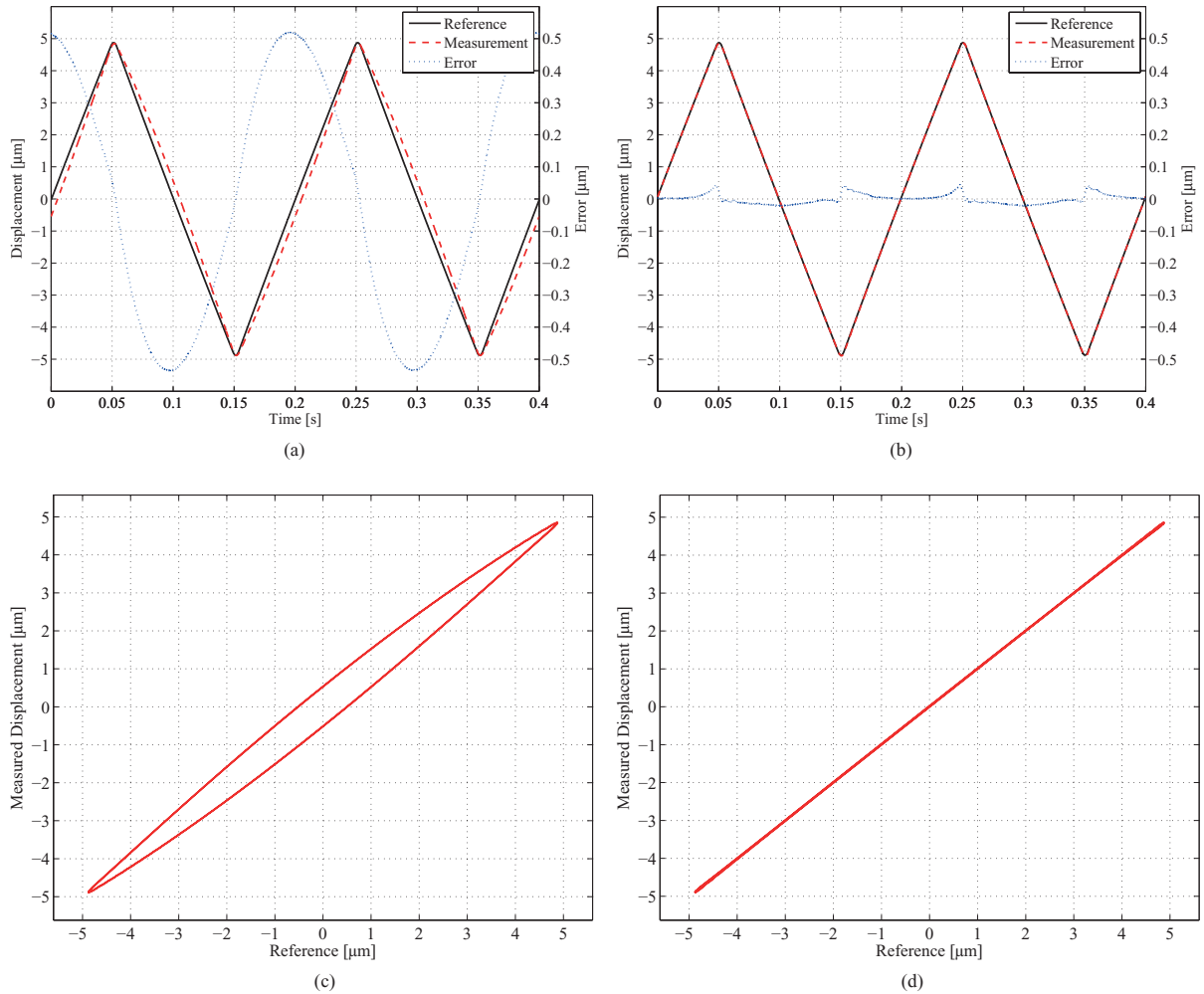

FIG. 4. Triangle-wave reference at 5 Hz with 5.0 μm amplitude (4.5 μm linear range). (a) Time-series for the reference signal, and the stationary measured displacement and error when using linear feed-forward. (b) Time-series for the reference signal, and the stationary measured displacement and error when using hysteresis compensation. (c) Reference-to-displacement map when using linear feed-forward. (d) Reference-to-displacement map when using hysteresis compensation.
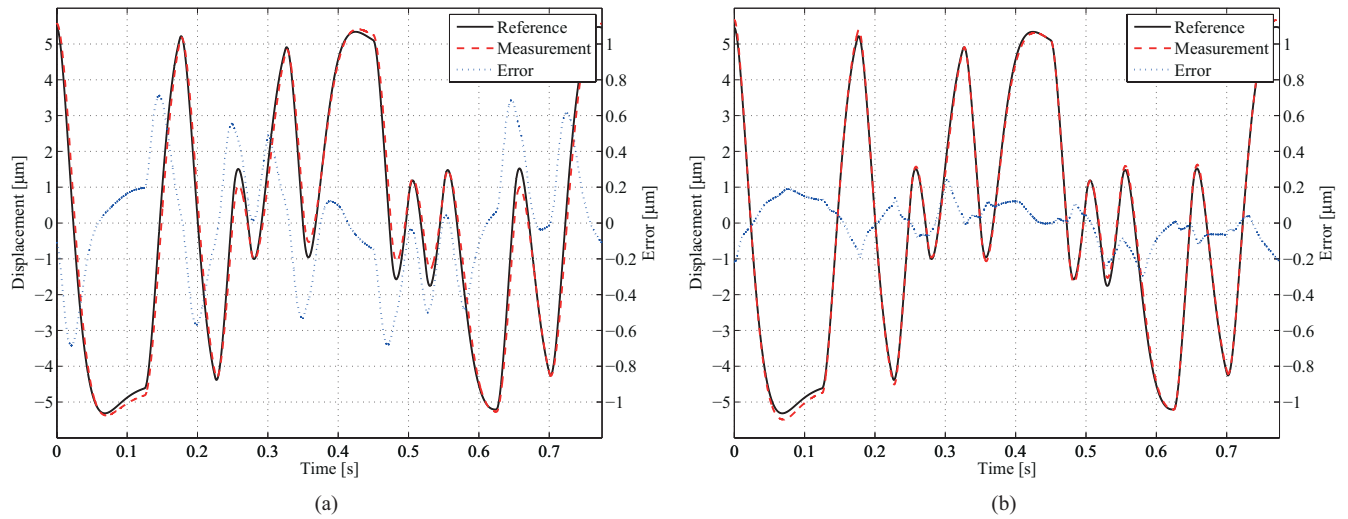
FIG. 5. Filtered PRBS reference. (a) Time-series for the reference signal, and the stationary measured displacement and error when using linear feed-forward. (b) Time-series for the reference signal, and the stationary measured displacement and error when using hysteresis compensation.

scaling amplifier from Stanford Research Systems. The capacitive measurement has a sensitivity of 1/5 V/μm and the voltage amplifier has a gain of 20 V/V. The programmable filters were used as reconstruction and anti-aliasing filters. The scaling amplifier was used to amplify the signal from the capacitive gauge in order to maximize the resolution of the quantized signal. With the DS1103 system, a sampling frequency of 50 kHz was used in all the experiments. For numerical integration, a third-order Runge-Kutta scheme (Bogacki-Shampine) was used.

The first part of the experiments were done using a triangle wave reference signal, where 10% of the signal was replaced by a smooth polynomial around the extremal points to reduce vibrations. A second set of experiments were done using a filtered pseudo random binary signal (PRBS). This signal had a length of 38 750 samples, a bandwidth of 40 Hz, a ±5 μm range, and was filtered by a second-order low-pass Butterworth filter with a 10 Hz cut-off frequency.

B. Experiments

The efficacy of the hysteresis model (1) and the parameter identification scheme presented in Sec. III B can be seen from Fig. 3. Here, a triangle-wave signal has been applied, but the response is very similar for any periodic input, which is monotonically increasing and decreasing between two extrema. Note that the observed hysteresis is highly symmetric, and the hysteresis model is therefore well suited to describe the response. Identified parameters for the hysteresis model can be found in Table I. As can be seen, the parameters depend on the input signal. The identified parameters appear to provide a good fit to the observed response, but there is some model discrepancy, especially at the extremal values where the input signal switches direction.

Figure 4(a) displays time-series for the reference, measured displacement, and the error when using the linear feed-forward scheme and a triangle-wave reference signal. Adapting the gain coefficient K makes it possible to match the ex-

tremal values of the measured response and the reference with very high accuracy, and the residual error is almost exclusively due to the hysteresis nonlinearity. The corresponding reference-to-displacement map is shown in Fig. 4(b). Note that despite the high accuracy in adapting the gain coefficient K, the hysteretic character of the response is clearly visible.

Applying the hysteresis compensation scheme proposed in Sec. III B, it can be seen from both the time-series plots in Fig. 4(c) and the reference-to-displacement map in Fig. 4(d) that there is a significant reduction in the error. The reduction in maximum error is approximately 90% from when applying a linear feed-forward scheme, to when applying the hysteresis compensation scheme. Most of the residual error when applying the hysteresis compensation scheme is due to the model discrepancy near the extremal values of the reference signal.

Assessing the performance under non-ideal conditions was done using the filtered PRBS reference. The continuous repetition of a PRBS sequence is a periodic signal, but for the duration of the sequence, it behaves as a non-periodic

TABLE II. Maximum stationary error when using linear feed-forward and the hysteresis compensation scheme.

Reference signal	Linear feed-forward		Hysteresis compensation		
	Absolute error (μm)	Relative error (%)	Absolute error (μm)	Relative error (%)	Error reduction (%)
2.5 μm @ 5.0 Hz	0.20	8.3	0.016	0.67	92
5.0 μm @ 2.5 Hz	0.54	11	0.055	1.1	90
5.0 μm @ 5.0 Hz	0.54	11	0.045	0.92	92
7.5 μm @ 5.0 Hz	0.93	13	0.053	0.72	94
Filtered PRBS	0.71	13	0.30	5.4	59

TABLE III. Maximum stationary error when using the hysteresis compensation scheme with parameter values found for a reference signal other than the one applied.

Reference signal	Absolute error (μm)	Relative error (%)	
2.5 μm @ 5.0 Hz	0.28	12	Using parameters found for 7.5 μm amplitude reference.
7.5 μm @ 5.0 Hz	0.67	9.2	Using parameters found for 2.5 μm amplitude reference.

signal, and the filtered signal is therefore not monotonically varying between only two extrema. The results for the linear feed-forward scheme are shown in Fig. 5(a), and the results when using the hysteresis compensation scheme are found in Fig. 5(b). The error obtained when using the hysteresis compensation scheme is still significantly lower than when using the linear feed-forward scheme, producing a reduction in maximum error of approximately 59%. It is apparent, however, that the effectiveness is reduced compared to when applying the triangle-wave signal.

The maximum errors observed for some different configurations of the reference signal are presented in Table II. The reduction in error is found as $100 \times (1 - e_h/e_l)$, where e_h and e_l are the maximal errors, $\max(|r - x|)$, when using the hysteresis compensation scheme, and linear feed-forward, respectively.

If the parameters of the hysteresis model applying the compensation scheme for a different signal than what the parameter were found for, the compensation scheme can produce very poor results. Error figures illustrating this are summarized in Table III. This suggests that the parameter identification scheme should be running while using the compensation scheme, or that hysteresis model parameters should be found for a family of reference signals, and that some form of gain scheduling should be used if a displacement measurement is not always available while using the equipment.

V. CONCLUSIONS

In this paper, a feed-forward hysteresis compensation scheme is proposed for piezoelectric actuators. The scheme is based on a reformulation of the Coleman-Hodgdon model, where the reformulation produces a mathematically equivalent input-output map. The original Coleman-Hodgdon model can be used for parameter identification, while the reformulation can be used to generate an estimate the hysteretic response and to linearize the input-output map. Since the parameters used in the scheme are identified online, the method will provide consistent performance, even when the hysteretic response changes due to different reference signals and other factors such as depolarization of the material and actuator temperature. The proposed method is well suited for the case of symmetric hysteretic responses and certain periodic reference trajectories. The method has low complexity and is thus readily applicable for real-time implementation. Experimental results are presented to illustrate the hysteresis compensation scheme. The experiments showed that the method re-

duced the hysteretic behavior of a piezoelectric actuator significantly, providing a reduction of more than 90% compared to when when assuming a linear response.

APPENDIX A: PARAMETER IDENTIFICATION

The least-squares method[16] is perhaps the best known method for parameter identification. It can be used in recursive and non-recursive form. It works by fitting experimental data to a given model by minimizing the sum of the squares of the difference between the computed response from the model and the actual measured response. Noise and disturbances in the measured signal is then expected to have less effect on the accuracy of the resulting parameter estimates.

Here, it is used in the recursive form to estimate the parameters, α, β, and γ, for the hysteresis model (1), and the linear gain coefficient K in (8).

The starting point is a model of the system, assuming the measured response z can be described as a vector of model parameters θ appearing affinely with a vector of known signals, φ, called the regressor:

$$z = \theta^{\mathrm{T}}\varphi. \tag{A1}$$

The objective of the method is to find a good estimate of the vector of parameter values, $\hat{\theta}$. By computing the estimated response

$$\hat{z} = \hat{\theta}^{\mathrm{T}}\varphi, \tag{A2}$$

the estimate error ϵ can be formed as

$$\epsilon = \frac{z - \hat{z}}{m^2}, \tag{A3}$$

where m^2 is a normalization signal (defined below). The least-squares estimate of the parameters is obtained by minimizing the cost-function

$$J(\hat{\theta}) = \frac{1}{2}\int_0^t e^{-\lambda(t-\tau)}\epsilon^2 m^2 \, d\tau + \frac{1}{2}e^{-\lambda t}(\hat{\theta} - \hat{\theta}_0)^{\mathrm{T}}Q_0(\hat{\theta} - \hat{\theta}_0), \tag{A4}$$

where a forgetting factor $\lambda > 0$ is introduced to discount past data in order to achieve exponential convergence. The matrix Q_0 is used to weigh the significance of the initial parameter estimates, $\hat{\theta}_0$, in minimizing the cost-function.

The above expressions can be used to derive both the recursive and the non-recursive forms of the least-squares method. Here, the recursive form is applied, as it is amenable to online implementation. The parameter update law is then given by

$$\dot{\hat{\theta}} = P\epsilon\varphi \,, \ \theta(0) = \theta_0. \tag{A5}$$

The matrix P is called the covariance matrix, and can be found by computing

$$\dot{P} = \begin{cases} \lambda P - \dfrac{P\varphi\varphi^{\mathrm{T}}P}{m^2}, & \text{if } \|P\| \leq R_0 \\ 0 & \text{otherwise} \end{cases}, \quad P(0) = Q_0^{-1}. \quad \text{(A6)}$$

The initial covariance matrix must be symmetric and positive definite, $P(0) = Q_0^{-1} = Q_0^{-\mathrm{T}} > 0$. By using the forgetting factor λ when updating the covariance P, there is a possibility for P to grow without bound. To avoid this, some norm on P, $\|P\|$, is not allowed to grow larger than R_0, by stopping the update of P by setting $\dot{P} = 0$. The initial covariance matrix should therefore also satisfy $\|P(0)\| \leq R_0$.

The normalization signal m^2 can be constructed in various ways. Here, it is taken to be

$$m^2 = 1 + n_s{}^2, \quad n_s{}^2 = \varphi^{\mathrm{T}}P\varphi. \quad \text{(A7)}$$

Normalization ensures boundedness of the signals used in the identification scheme.

This method is referred to as modified least-squares with forgetting factor. It has the properties $\epsilon, \epsilon n_s, \hat{\theta}, \dot{\hat{\theta}}, P \in \mathcal{L}_\infty$, and $\epsilon, \epsilon n_s, \dot{\hat{\theta}} \in \mathcal{L}_2$. In addition, if the regressor φ is persistently exciting (PE), then $\hat{\theta}$ converges exponentially to θ. A piecewise continuous signal vector $\varphi : \mathbb{R}^+ \to \mathbb{R}^n$ is said to be PE in $\mathbb{R}^n$ with a level of excitation $\alpha_0 > 0$ if there exist constants $\alpha_1, T_0 > 0$ such that

$$\alpha_1 I \geq \frac{1}{T_0} \int_t^{t+T_0} \varphi\varphi^{\mathrm{T}} \, d\tau \geq \alpha_0 I, \quad \forall t \geq 0. \quad \text{(A8)}$$

For the system at hand, the input signal u and the time derivative $\dot{u}$ are known, as u is generated by the expression (11), and by using a reference signal that is differentiable, i.e., r and $\dot{r}$ being known and bounded. The displacement x is measured by the capacitive probe, and the time derivative of this signal is needed to identify the parameters for the hysteresis model. To avoid pure numerical differentiation, the output $z = \dot{w} = \dot{x}$ and regressor vector φ was in this case filtered using proper filters, that is, $\bar{z}(s) = s W_p(s) x(s)$, and $\bar{\varphi}(s) = W_p(s)\varphi(s)$, where $W_p(s)$ is a first-order low-pass filter with a 2.5 kHz cut-off frequency. Pure numerical differentiation is not desired as it will amplify measurement noise, degrading the performance of the identification scheme. If the measured signal x contains a bias component, filtering $\bar{z}$ and $\bar{\varphi}$ by identical high-pass filters with a cut-off frequency lower than the lowest frequency component in the input signal u can be used to improve estimates.

APPENDIX B: DERIVATION OF THE ALTERNATIVE VERSION OF THE COLEMAN-HODGDON MODEL

Equation (1) can be solved explicitly, by observing that is can be written as

$$\dot{w} = (\beta - \alpha w + \gamma u)(\dot{u})^+ - (\beta + \alpha w - \gamma u)(\dot{u})^-, \quad \text{(B1)}$$

where $(\dot{u})^+ = \dot{u}$ and $(\dot{u})^- = 0$ when $\dot{u} \geq 0$, and $(\dot{u})^+ = 0$ and $(\dot{u})^- = \dot{u}$ when $\dot{u} < 0$. The dependence on time can then be cancelled. What is left are two linear differential equations for

the two cases. For the case $\dot{u} \geq 0$, the solution of

$$dw = (\beta - \alpha w + \gamma u) \, du \Rightarrow \frac{dw}{du} + \alpha w = \beta + \gamma u \quad \text{(B2)}$$

can be found as

$$w = e^{-h} \left[\int e^h (\beta + \gamma u) \, du + C_1 \right], \quad \text{(B3)}$$

$$= e^{-\alpha u} \left[\frac{(\alpha\beta - \gamma + \alpha\gamma u)e^{\alpha u}}{\alpha^2} + C_1 \right], \quad \text{(B4)}$$

where $h = \int \alpha \, du = \alpha u$ has been used. This yields

$$w^+ = \frac{\gamma}{\alpha} u + \frac{\alpha\beta - \gamma}{\alpha^2} + C_1 e^{-\alpha u}, \quad \text{(B5)}$$

where

$$w_0 = \frac{\gamma}{\alpha} u_0 + \frac{\alpha\beta - \gamma}{\alpha^2} + C_1 e^{-\alpha u_0}$$

$$\Rightarrow C_1 = e^{\alpha u_0} \left(w_0 - \frac{\alpha\beta - \gamma}{\alpha^2} - \frac{\gamma}{\alpha} u_0 \right). \quad \text{(B6)}$$

Similarly, for the case $\dot{u} < 0$, the solution is

$$w^- = \frac{\gamma}{\alpha} u + \frac{\gamma - \alpha\beta}{\alpha^2} + C_2 e^{\alpha u}, \quad \text{(B7)}$$

where

$$C_2 = e^{-\alpha u_0} \left(w_0 - \frac{\gamma - \alpha\beta}{\alpha^2} - \frac{\gamma}{\alpha} u_0 \right). \quad \text{(B8)}$$

The solutions (B5) and (B7), can be put on the form

$$w = \frac{\gamma}{\alpha} u + w_h, \quad \text{(B9)}$$

which is the form in (2), where w_h accounts for the hysteretic behavior. As it happens, w_h can be taken to be the solution of the differential equation in (3), which is

$$\dot{w}_h = -b\dot{u} - a w_h |\dot{u}|. \quad \text{(B10)}$$

The parameters of this formulation are related to the parameters in (1) by

$$a = \alpha, \quad b = \frac{\gamma - \alpha\beta}{\alpha}, \quad \text{and } c = \frac{\gamma}{\alpha}. \quad \text{(B11)}$$

Equation (3) is similar to a case of the well known Dahl solid friction model,[17] except for the sign of the parameter b. This equation can also be solved for the cases $\dot{u} \geq 0$ and $\dot{u} < 0$ in a similar fashion as above, using, e.g., separation of variables. The solution for $\dot{u} \geq 0$ is

$$w_h^+ = \frac{1}{a}(-b - C_3 e^{-au}) = \frac{\alpha\beta - \gamma}{\alpha^2} - \frac{1}{\alpha} C_3 e^{-\alpha u}, \quad \text{(B12)}$$

where

$$C_3 = e^{au_0}(-b - a w_{h0})$$

$$= -\alpha e^{\alpha u_0} \left(w_0 - \frac{\alpha\beta - \gamma}{\alpha^2} - \frac{\gamma}{\alpha} u_0 \right) = -\alpha C_1, \quad \text{(B13)}$$

and for $\dot{u} < 0$ it is

$$w_h^- = \frac{1}{a}(b - C_4 e^{au}), \quad \text{(B14)}$$

where

$$C_4 = e^{-au_0}(b - a w_{h0}) = -\alpha C_2. \quad \text{(B15)}$$

By substitution of (B12) and (B14) into (B9) and using the relations in (B11), it can be seen that the two formulations are equivalent, by comparison to (B5) and (B7).

APPENDIX C: DERIVATION OF THE HYSTERESIS COMPENSATION SCHEME

As was shown in Sec. III B, by applying the input (14), i.e.,

$$u_h = \frac{K}{c}u - \frac{1}{c}\hat{w}_h, \tag{C1}$$

using an estimate of w_h, the effect of the hysteresis can be cancelled.

An open-loop observer to estimate w_h can be obtained from (3), substituting u_h for the input u, which results in (16), that is,

$$\dot{\hat{w}}_h = -b\dot{u}_h - a\hat{w}_h\,|\dot{u}_h|$$
$$= -b\left(\frac{K}{c}\dot{u} - \frac{1}{c}\dot{\hat{w}}_h\right) - a\hat{w}_h\left|\frac{K}{c}\dot{u} - \frac{1}{c}\dot{\hat{w}}_h\right|. \tag{C2}$$

This expression can be rewritten as

$$\dot{\hat{w}}_h = \begin{cases} K\frac{-a\hat{w}_h - b}{-a\hat{w}_h - b + c}\dot{u}, & \dot{u}_h \geq 0 \\ K\frac{a\hat{w}_h - b}{a\hat{w}_h - b + c}\dot{u}, & \dot{u}_h < 0 \end{cases}, \tag{C3}$$

but the switching criterion cannot be determined causally, as it is dependent on $\dot{u}_h$ and not $\dot{u}$.

The expression (C3) can again be solved explicitly by separation of variables by canceling the dependence on time. For the case $\dot{u}_h \geq 0$,

$$\frac{d\hat{w}_h^+}{du} = K\frac{-a\hat{w}_h^+ - b}{-a\hat{w}_h^+ - b + c}, \tag{C4}$$

which solution is found as

$$\hat{w}_h^+ - \frac{c}{a}\ln\left(a\hat{w}_h^+ + b\right) = Ku + C_5, \tag{C5}$$

where

$$C_5 = \hat{w}_{h0} - \frac{c}{a}\ln\left(a\hat{w}_{h0} + b\right) - Ku_0. \tag{C6}$$

This implicit equation can be solved explicitly for $\hat{w}_h$ as a function of u by using the Lambert W function,[18] denoted $W(\cdot)$:

$$\hat{w}_h^+ = -\frac{c}{a}W\left(-\frac{1}{c}\exp\left(-\frac{aKu + aC_5 + b}{c}\right)\right) - \frac{b}{a}. \tag{C7}$$

Similarly, for the case $\dot{u}_h < 0$,

$$\hat{w}_h^- + \frac{c}{a}\ln\left(-a\hat{w}_h^- + b\right) = Ku + C_6, \tag{C8}$$

where

$$C_6 = \hat{w}_{h0} + \frac{c}{a}\ln\left(-a\hat{w}_{h0} + b\right) - Ku_0, \tag{C9}$$

and the explicit solution is found as

$$\hat{w}_h^- = \frac{c}{a}W\left(-\frac{1}{c}\exp\left(\frac{aKu + aC_6 - b}{c}\right)\right) + \frac{b}{a}. \tag{C10}$$

Now, differentiating (C7) or (C10) by u yields

$$\frac{d\hat{w}_h}{du} < 0, \tag{C11}$$

in either case. Thus, since

$$\frac{d\hat{w}_h}{du} = \frac{\dot{\hat{w}}_h}{\dot{u}}, \tag{C12}$$

$\dot{u} \geq 0 \Rightarrow \dot{\hat{w}}_h \leq 0$, and $\dot{u} \leq 0 \Rightarrow \dot{\hat{w}}_h \geq 0$. Therefore, $\dot{u}_h \geq 0 \Rightarrow \dot{u} \geq 0$ and $\dot{u}_h < 0 \Rightarrow \dot{u} < 0$. This shows that (C3) is equivalent to (17).

[1]S. Devasia, E. Eleftheriou, and S. O. R. Moheimani, IEEE Trans. Control Syst. Technol. **15**, 802 (2007).

[2]G. M. Clayton, S. Tien, K. K. Leang, Q. Zou, and S. Devasia, ASME J. Dyn. Syst., Meas., Control **131**, 061101 (2009).

[3]S. Hudlet, M. S. Jean, D. Royer, J. Berger, and C. Guthmann, Rev. Sci. Instrum. **66**, 2848 (1995).

[4]D. Berlincourt, B. Jaffe, H. Jaffe, and H. Krueger, IEEE Trans. Ultrason. Eng. **7**, 1 (1960).

[5]C. Lee and S. M. Salapaka, Nanotechnology **20**, 035501 (2008).

[6]J. Doyle, B. Francis, and A. Tannenbaum, *Feedback Control Theory* (Macmillan, 1992).

[7]S. Boyd and C. Barratt, *Linear Controller Design: Limits of Performance* (Prentice-Hall, 1991).

[8]K. Leang, Q. Zou, and S. Devasia, IEEE Control Syst. **29**, 70 (2009).

[9]R. Iyer and X. Tan, IEEE Control Syst. **29**, 83 (2009).

[10]S. Devasia, IEEE Trans. Autom. Control **47**, 1865 (2002).

[11]C. V. Newcomb and I. Flinn, Electron. Lett. **18**, 442 (1982).

[12]A. J. Fleming and K. K. Leang, Ultramicroscopy **108**, 1551 (2008).

[13]R. Banning, W. de Koning, H. Adriaens, and R. Koops, Automatica **37**, 1883 (2001).

[14]B. D. Coleman and M. L. Hodgdon, Int. J. Comput. Eng. Sci. **24**, 897 (1986).

[15]ANSI/IEEE Std 176-1987 (1988).

[16]P. A. Ioannou and J. Sun, *Robust Adaptive Control* (Prentice-Hall, 1996).

[17]P. R. Dahl, "A solid friction model", Tech. Rep., The Aerospace Corporation, El Segundo, California 90245, 1968.

[18]R. M. Corless, G. H. Gonnet, D. E. G. Hare, D. J. Jeffrey, and D. E. Knuth, Adv. Comput. Math. **5**, 329 (1996).